Metastases arise as new cancers from cells of target organs transformed by cell-free chromatin particles released from dying cancer cells

Gorantla V. Raghuram[1,2], Kavita Pal[1,2], Soniya Shende[1,2], Naveen Kumar Khare[1,2], Vishalkumar Jadhav[1,2], Sushma Shinde[1,2], Ratnam Prasad[1,2], Harshada Wani[1,2], Indraneel Mittra[1,2,*]

[1]Translational Research Laboratory, Tata Memorial Centre, Advanced Centre for Treatment Research and Education in Cancer,
Kharghar, Navi Mumbai – 410210, India
[2]Homi Bhabha National Institute, Anushakti Nagar, Mumbai - 400 094, India

* Corresponding author: imittra@actrec.gov.in

Abstract

Based on our earlier report that cell-free chromatin particles (cfChPs) released from dying cancer cells are potentially oncogenic, we hypothesised that metastases arise as new cancers from the cells of target organs transformed by cfChPs released from dying cancer cells. We intravenously injected MDA-MB-231 human breast cancer cells and A375 human melanoma cells into mice with severe combined immunodeficiency and observed that the cells died upon reaching the lungs, and released cfChPs that accumulated in the lung cell nuclei at 48 h. We detected the activation of 10 hallmarks of cancer and immune checkpoints in lung cells at 72 h, suggesting that the lung cells had rapidly transformed into incipient cancer cells. Metaphase preparations and single-cell clones developed from cell cultures of lung metastases that subsequently developed contained chimeric chromosomes of both mouse and human DNA, and the cells co-expressed both human- and mouse-specific proteins. Intravenous injection of purified cfChPs isolated from radiation-killed MDA-MB-231 cells induced lung metastasis containing chimeric chromosomes and co-expressing proteins, providing direct evidence that cfChPs are involved in metastasis induction. These findings strongly support our hypothesis that metastases arise from the cells of target organs and not from cells derived from the primary tumour.

Introduction

Metastasis is a complex process and the leading cause of cancer-related deaths. Despite extensive research over many decades, the mechanisms underlying the multiple steps involved in the metastatic cascade remain poorly understood[1,2]. For example, it is not clear how detached tumour cells that enter the circulation escape immune surveillance by natural killer cells, T cells, and macrophages[3], or how the extravasated cells withstand the circulatory shearing forces[4]. It is also not understood how cancer cells navigate vascular capillaries that have an average diameter of ~5 µm[5] when the tumour cells themselves are >20 µm in size[1,5]. Above all, how cancer cells pass through the blood-brain barrier to intravasate into the brain and survive in an inhospitable environment, to grow and develop into a metastasis, lacks a rational explanation[6,7]. Hence, the prevailing theory of cancer metastasis requires re-evaluation, and new ideas are needed[8,9].

The symbiotic influence of two deeply entrenched theories has dominated metastasis research for decades. The first theory suggests that metastatic tumours are histologically similar to the underlying primary tumours. Although this theory has not been scientifically tested, it continues to form the conceptual foundation of metastatic research. A recent study that evaluated this theory in a blinded experiment raised doubts about its veracity[10]. Nonetheless, this entrenched theory prompted the formulation of a second theory, which posits that cells leaving the primary tumour enter the circulation and travel to distant organs where they colonise to form metastases that are histologically similar to the primary tumour. The striking finding of Fidler[11] that 99% of cancer cells injected intravenously into mice die by the time they reach distant target organs was construed to suggest that the remaining 1% surviving cells are responsible for inducing metastasis.

This conjecture led to the emergence of the theory of “metastatic inefficiency”[12,13], which ensured that the two entrenched theories remained unchallenged. The possibility that the 99% of the cells that die may have consequences for the development of metastasis remains unaddressed.

An alternative theory of metastasis proposes that nucleic acids released from dying cancer cells and transported via the circulation to distant sites can transform the cells of target organs to generate new tumours that masquerade as metastasis[14–19]. In line with this alternative theory, in the present study, we show that intravenously injected human cancer cells into mice rapidly die upon reaching the lungs and release chromosomal fragments in the form of cell-free chromatin particles (cfChPs) that accumulate in the nuclei of lung cells. This leads to the activation of 10 hallmarks of cancer and the immune checkpoint PD-L1 as early as 72 h following injection, suggesting that the lung cells were rapidly transformed into incipient cancer cells. The subsequently developed metastases were genetically chimeric and contained both mouse- and human-specific DNA, indicating that the cfChPs of human origin integrated into the genomes of mouse lung cells and were involved in the process of metastasis. The fact that cfChPs from dying cancer cells were the agents responsible for transforming lung cells into metastases was strongly suggested by the demonstration that the intravenous injection of purified cfChPs isolated from radiation-killed human cancer cells also generated lung metastases and harboured chimeric genomes. These findings lead us to conclude that lung metastases arise as new cancers from mouse lung cells transformed with cfChPs released from dying human cancer cells.

Methods

Ethics approval

The experimental protocol was approved by the Institutional Animal Ethics Committee (IAEC) of the Advanced Centre for Treatment, Research, and Education in Cancer (ACTREC), Tata Memorial Centre (TMC), Navi Mumbai, India. The experiments were conducted in compliance with the ethical regulations and humane endpoint criteria of the IAEC and ARRIVE guidelines.

Mice

Inbred female non-obese diabetic (NOD) mice (NOD.Cg-Prkdcscid/J) with severe combined immunodeficiency (SCID) were used in this study. They were obtained from the Institutional Animal Facility, maintained according to IAEC standards, and housed in pathogen-free cages containing husk bedding under a 12-h light/dark cycle with free access to water and food. A HVAC system was used to control room temperature, humidity, and air pressure. The ACTREC-IAEC maintains respectful treatment, care, and use of animals in scientific research and aims to contribute to the advancement of knowledge following ethical and scientific necessity. All scientists and technicians involved in this study underwent training in the ethical handling and management of animals under the supervision of Federation of European Laboratory Animal Science Associations (FELASA)-certified attending veterinarians. The animals were euthanised at appropriate time points in a CO_2 atmosphere by cervical dislocation under the supervision of FELASA-trained animal facility personnel.

Cell culture

We used two human cancer cell lines: MDA-MB-231 (human breast cancer) and A375 (human malignant melanoma). Cells were obtained from the American Type Culture Collection (ATCC) and grown in Dulbecco's modified Eagle medium (DMEM) with 10% fetal bovine serum (FBS) + 1% antibiotic cocktail in an atmosphere of 5% CO_2 and 100% humidity.

Fluorescent dual-labelling of cells

The MDA-MB-231 and A375 cells were dually labelled in their DNA and histones according to a protocol previously described by us[18]. Briefly, cells were plated at a density of 6×10^4, and after overnight culture (cell count ~1×10^5), their DNA and histones were labelled with BrdU and histone 2BGFP, respectively. BrdU labelling was performed for 24 h using 10 μM BrdU (Sigma Chemicals, St. Louis, MO, USA; Catalogue No. B5002). Histone H2B labelling was performed for 36 h using CellLight® Histone 2BGFP (Thermo Fisher Scientific, Waltham MA, USA; Catalogue No. C10594). Representative images of the fluorescently double-labelled MDA-MB-231 and A375 cells are shown in Fig. 1a.

Intravenous injection and detection of fluorescently dual-labelled particles in lung cells

Dually labelled MDA-MB-231 and A-375 cells (1×10^5) were intravenously injected into SCID mice, and the animals were sacrificed after 48 h. The lungs were harvested and cryosections were prepared for immunofluorescence (IF) staining with an anti-BrdU antibody, as described previously (Abcam, Cambridge, UK; Catalogue no. ab70328)[19]. Images were acquired and analysed using an Applied Spectral Bioimaging System (ASI, Israel).

Detection of hallmarks of cancer in lung cells

One hundred thousand unlabelled MDA-MB-231 cells were intravenously injected into SCID mice, while control SCID mice were injected with saline. Mice in both groups were sacrificed at 72 h, the lungs were harvested, and cryosections were prepared for IF analysis to detect the hallmarks of cancer, as defined by Hanahan and Weinberg[20]. Antibodies against 13 biomarkers representing 10 hallmarks were used in the analysis. Details of the antibodies used are provided in Supplementary Table 1 B and 1C. IF analysis was performed as previously described by us[18]. Images were acquired and analysed using an Applied Spectral Bioimaging System (ASI, Israel).

Detection of lung metastasis

The MDA-MB-231 and A375 cells induce lung metastasis when injected intravenously into SCID mice[21,22]. Ten SCID mice were intravenously injected with 1×10^5 MDA-MB-231 cells, and five mice were injected with an equal number of A375 cells. Two mice from the MDA-MB-231 group and one mouse from the A375 group were euthanised on days 37, 51, 76, 112, and 125. Formalin-fixed paraffin-embedded (FFPE) sections of the lungs were prepared, stained with haematoxylin and eosin (H&E), and examined for the histological detection of metastases. In the MDA-MB-231 group, grade III metastases were detected on day 112 in two mice and on day 125 in two mice (total number of metastases 4/10). One of the tumours detected on day 112 was used for fluorescence in situ hybridisation (FISH) analysis, and the other was used for preparing primary cultures. In the A375 group, grade III metastases were detected in one mouse each on days 76, 112, and 125 (number of metastases 3/5). The tumour detected on day 76 was used for FISH analysis and that detected on day 112 was used to prepare primary cultures.

Representative H&E images of MDA-MB-231 and A375 lung metastases are shown in Supplementary Fig. 1.

Development of primary cultures and single-cell clones

Lung metastases which were visible as white patches on the lung surface were carefully excised under aseptic conditions, minced with scalpel followed by collagenase I treatment (1mg/ml) for 30 min at 37^0C with gentle shaking. The dissociated cells were centrifuged, washed X 2 with PBS and plated in $65mm^3$ petri dishes containing DMEM with 20% fetal bovine serum (FBS) + 1% antibiotic cocktail. The medium was changed after 24hr and cells were allowed to grow to confluency and passaged several times. After the 3-4 passages foci of the transformed cells became visible. Cells at the foci were carefully picked, trypsinised, and subcultured in the above medium. Single-cell clones were prepared from primary cultures using the serial dilution method and were used for further analysis. The primary culture and single-cell clones were verified for their epithelial origin using a recombinant anti-EpCAM antibody (EPR20533-63; Catalogue number: ab221552, Abcam; Supplementary Fig. 2).

Detection of species-specific DNA in lung metastasis by FISH

Unstained FFPE sections of metastatic tumours were processed for FISH analysis using mouse (green) or human (red)-specific whole genomic DNA probes (custom synthesised by ASI, Israel) as described by us previously[18] (Supplementary Table 1A). Images were acquired and analysed using an Applied Spectral Bioimaging System (ASI, Israel). At the outset, we performed extensive control experiments to ensure that the human and mouse FISH probes did not cross-react (Supplementary Fig. 3).

Detection of species-specific proteins in lung metastasis by IF

Unstained FFPE sections of metastatic tumours were processed for IF analysis using mouse- and human-specific antibodies (green and red, respectively) and appropriate secondary antibodies. We used species-specific monoclonal antibodies (mAbs), namely, HLA class 1-ABC, which is unique to humans, and MHC class II, which is unique to mice. Initially, we performed elaborate control experiments to ensure that the human and mouse mAbs did not cross-react (Supplementary Fig. 3). The details of the antibodies used are provided in Supplementary Table 1B and 1C.

Isolation of cfChPs from irradiated dying cancer cells

The MDA-MB-231 and A375 cells grown in DMEM containing 10% foetal bovine serum were plated at a density of 1.5×10^6 in 10 cm culture dishes. The following day (cell density ~3×10^6), cells were irradiated with γ rays (10 Gy) and incubated for 72 h. Floating cells in the supernatant were collected by centrifugation and used for cfChP isolation as described in detail by us previously[18]. An electron microscopy image of cfChPs isolated from the MDA-MB-231 cells is shown in Supplementary Fig. 4.

Intravenous injection of purified cfChPs into SCID mice

Five SCID mice were intravenously injected with 700 ng cfChPs isolated from dying MDA-MB-231 cells, and four mice were intravenously injected with cfChPs isolated from dying A375 cells (2/4 mice in the A375 group subsequently died). The animals were sacrificed after 150 days, and H&E sections of their lungs were examined for the development of metastases. Two out of five mice from the MDA-MB-231 group and 0 / 2 from the A375 group harboured lung metastases. A representative H&E image of lung metastasis that developed following the intravenous injection of cfChPs isolated from MDA-MB-231 cells

is shown in Supplementary Fig. 5. FFPE sections were prepared and processed for FISH and IF as described above.

Statistical analysis

Statistical analysis pertains to the 13 cancer hallmark biomarkers mentioned above. The mean (± SEM) values of biomarkers in the control and MDA-MB-231-injected groups were individually compared using two tailed Student's t test. A combined analysis of the median values of all 13 biomarkers in control and MDA-MB-231 injected groups was performed using the Mann–Whitney U test (see the legend to Figure 2). Analyses were performed using GraphPad Prism Version 6.0. The threshold for statistical significance was set at $p<0.05$.

Results

Detection of fluorescently dually labelled cfChPs in the nuclei of lung cells

IF analysis of cryosections of lungs of mice injected with fluorescently dual-labelled MDA-MB-231 and A375 cells revealed copious accumulation of co-localising red and green fluorescent signals indicative of cfChPs in the nuclei of lung cells (Fig. 1b). This suggests, in agreement with the report by Fidler[11], that injected MDA-MB-231 and A375 cells died upon reaching the lungs and released cfChPs that accumulated in the lung cell nuclei. Notably, no intact double-labelled MDA-MB-231 or A375 cells were detected in the lungs.

Intravenously injected cancer cells upregulate the hallmarks of cancer in lung cells

IF analysis of cryosections of lungs of mice injected with (unlabelled) MDA-MB-231 cells at 72 h showed marked activation of all 13 biomarkers representing 10 hallmarks of cancer (Fig. 2a and Supplementary Fig. 6). When compared statistically, 11 out of 13

biomarkers were found to be statistically significant; the exceptions were PDL-1 and TNF-α. A combined statistical analysis of all 13 hallmark biomarkers in the two groups revealed that the median value in the MDA-MB-231 injected groups was nearly eight-fold higher than that in the saline-injected controls (Fig. 2b). This finding indicated that the nuclear accumulation of cfChPs rapidly transformed mouse lung cells into incipient cancer cells by 72 h.

Lung metastases contain both mouse- and human-specific DNA

Metastases detected on day 112 in MDA-MB-231 injected mice and on day 78 in A375 injected mice were used for FISH analysis. FFPE sections were examined by dual FISH by simultaneously using both mouse- and human-specific whole-genome probes. Fluorescence microscopy revealed that the nuclei of all the tumour cells contained both mouse- and human-specific DNA (Fig. 3a). No nuclei stained exclusively with human DNA, as would be expected had the metastases arisen from intact MDA-MB-231 or A375 cells. This suggests that the cfChPs that accumulated in the lung cell nuclei were involved in the development of lung metastasis.

Lung metastases express both human- and mouse-specific proteins

The FFPE tumour sections were immune-stained with monoclonal antibodies against species-specific mouse and human proteins (MHC-II and HLA-ABC, respectively). The fluorescent signals of MHC-II and HLA-ABC were co-expressed in the same tumour cells, indicating that they expressed both human and mouse proteins (Fig. 3b). We concluded that HLA-ABC genes carried by cfChPs were being expressed in the mouse lung metastasis cells.

Metastatic tumour cells contain chimeric chromosomes

Metaphase spreads prepared from primary cultures of MDA-MB-231- and A375-induced lung metastases, and single-cell clones developed therefrom (MG6 and AG5, respectively), were examined by dual FISH i.e. simultaneous use of human- and mouse-specific whole genomic probes. Both the primary cultures and the MG6 and AG5 clones revealed chimeric chromosomes with the chromosomal arms containing both human and mouse DNA (Fig. 4a and 4b). The presence of human DNA in mouse chromosomes indicated that human cfChPs derived from dying MDA-MB-231 and A375 cells had integrated and fused with mouse cell chromosomes.

Metastatic tumour cells in culture express both human and mouse proteins

Primary cultures of MDA-MB-231 and A375 cells induced metastasis, and MG6 and AG5 clones, were simultaneously immune-stained with monoclonal antibodies against MHC-II and HLA-ABC. Fluorescence microscopy revealed that the same cultured tumour cells expressed both human- and mouse-specific proteins (Fig. 5a and 5b). This clearly indicated that the human HLA-ABC gene carried via cfChPs to integrate into the mouse lung cell genome aberrantly expressed the human-specific HLA-ABC protein in the metastatic tumour cells of the mouse lung.

cfChPs isolated from radiation-killed MDA-MB-231 cells induce lung metastasis

As mentioned in the Methods section, two of five mice injected with cfChPs isolated from radiation-killed MDA-MB-231 cells developed lung metastases on day 150 (Supplementary Fig. 5). When FFPE sections of the tumours were analysed with the simultaneous use of human and mice specific whole genomic probes, DNA signals specific to both species were detected in the tumour cell nuclei, with a preponderance of

mouse DNA (Fig. 6a). Co-localisation of mouse and human DNA signals in the same lung cell nuclei was clearly observed, indicating that the human cfChPs isolated from radiation-killed MDA-MB-231 cells had integrated into the mouse cell genome and were involved in the development of lung metastasis. Co-expression of human- and mouse-specific protein signals were also detected indicating that the same cells expressed both species-specific proteins (Fig. 6b).

An unexpected and incidental finding was that of a tumourous outgrowth in the thymus region of three cfChP-injected mice (one out of five mice from the MDA-MB-231 group and both mice from the A375 group; Supplementary Fig. 7). On H&E-stained sections, these tumours exhibited a highly undifferentiated pathology that precluded identification of their tissue origin (Supplementary Fig. 7). Nonetheless, FISH detected both human- and mouse-specific DNA in the same tumour cells, indicating that they had been transformed by the genomic integration of cfChPs isolated from radiation-killed human cells (Supplementary Fig. 7). IF analysis also showed that the tumour cells co-expressed both HLA-ABC and MHC-II proteins (Supplementary Fig. 7).

Discussion:

Consistent with Fidler's[11] report that most cancer cells intravenously injected into mice die within 24 h of reaching the target organs, we found that the injected MDA-MB-231 and A357 cells also died upon reaching the lungs of the injected mice. This was indicated by the detection of numerous fluorescently double labelled cfChPs in the nuclei of lung cells at 48 h. We also detected marked activation of 10 hallmarks of cancer in lung cells, indicating that cfChPs had rapidly transformed the mouse lung cells into incipient cancer

cells. This finding is consistent with our recent report showing that cfChPs released from dying cancer cells activate cancer hallmarks in bystander cells[23].

When incipient cancer cells formed histologically detectable metastatic lung tumours after 2–3 months, they contained both human and mouse specific DNA. No intact injected tumour cells containing exclusively human DNA were detected. The latter is expected to hold true for the current theory of cancer metastasis. Cells of primary cultures derived from metastatic tumours and single-cell clones developed therefrom contained chimeric chromosomes resulting from the fusion of human and mouse DNA, indicating that cfChPs from dying human cancer cells had amalgamated with the genomes of mouse lung cells. We further demonstrated that the genes contained within the chimeric chromosomes were expressed such that the metastatic tumour cells co-expressed both human- and mouse-specific proteins. Conclusive evidence that cfChPs from dying cells were responsible for the formation of lung metastases came from our demonstration that the intravenous injection of purified cfChPs isolated from radiation-killed MDA-MB-231 cells led to the development of lung metastases. The latter contained both mouse and human DNA and expressed both mouse- and human-specific proteins. Taken together, the above results lead to the conclusion that metastases arose from resident mouse lung cells resulting from the genomic integration of cfChPs released from the injected human cancer cells.

Numerous studies have examined the relationship between primary and metastatic tumours at the genomic level. Overall, the results have been conflicting, with multiple studies reporting concordance[24–27] and others reporting discordance[28–31] between the profiles of primary and metastatic tumours. Significant similarities and differences in gene

expression patterns have also been reported[32–37]. Studies investigating clonal evolution of metastases have also reported conflicting results. A wide repertoire of somatic changes in driver genes were reported which were either unique to the primary tumour or to the metastases or to be present in both[38–45]. Our finding that metastatic tumours contained DNA of both mouse and human origins and expressed both mouse and human proteins may help reconcile the above conflicting reports by suggesting that genetic signatures and gene expression patterns of both primary tumour cells and those of the target organs are to be expected in metastatic tumours. Conflicting reports in the literature may reflect the inherent bias of investigators when interpreting their results.

Our study could be criticized on the ground that we have depended largely on immunofluorescence data, and that it would have benefited from genomic and proteomic analyses to corroborate our findings. Such investigations could have elucidated on the existing conflicting reports with respect to the genomic and transcriptomic literature alluded to above. Nonetheless, the results of this study, in combination with our previous work in the field, provide an alternative model to understand the fundamental pathophysiology of metastatic cancer, in which metastases arise from the cells of the target organs and implicate cfChPs released from dying circulating tumour cells. The alternative model of metastasis is graphically illustrated in Fig. 7. It is increasingly recognised that all forms of cancer treatment, namely, chemotherapy, radiotherapy, and surgery, mobilise tumour cells into the circulation and potentially contribute to metastatic dissemination.[46-52] Therefore, to prevent iatrogenic morbidity and mortality, it is imperative to re-examine the currently accepted mechanisms of cancer metastasis so that appropriate therapeutic approaches can be developed to prevent cancer dissemination.

This is likely to require a re-examination of the currently used modalities of cancer treatment. Before such a fundamental change occurs, however, further corroborative evidence in clinical settings is required to confirm the findings reported in the current study.

References

1. Chambers, A. F., Groom, A. C. & MacDonald, I. C. Dissemination and growth of cancer cells in metastatic sites. *Nat. Rev. Cancer* **2**, 563–572 (2002).

2. Lambert, A. W., Pattabiraman, D. R. & Weinberg, R. A. Emerging Biological Principles of Metastasis. *Cell* vol. 168 at https://doi.org/10.1016/j.cell.2016.11.037 (2017).

3. Schaller, J. & Agudo, J. Metastatic colonization: Escaping immune surveillance. *Cancers* vol. 12 at https://doi.org/10.3390/cancers12113385 (2020).

4. Wirtz, D., Konstantopoulos, K. & Searson, P. C. The physics of cancer: the role of physical interactions and mechanical forces in metastasis. *Nat. Rev. Cancer* **11**, 512–522 (2011).

5. Potter, R. F. & Groom, A. C. Capillary diameter and geometry in cardiac and skeletal muscle studied by means of corrosion casts. *Microvasc. Res.* **25**, (1983).

6. Wilhelm, I., Molnár, J., Fazakas, C., Haskó, J. & Krizbai, I. A. Role of the blood-brain barrier in the formation of brain metastases. *Int. J. Mol. Sci.* **14**, 1383–1411 (2013).

7. Tiwary, S. *et al.* Metastatic brain tumors disrupt the blood-brain barrier and alter lipid metabolism by inhibiting expression of the endothelial cell fatty acid transporter Mfsd2a. *Sci. Rep.* **8**, (2018).

8. Weinberg, R. A. Coming full circle - From endless complexity to simplicity and back again. *Cell* vol. 157 at https://doi.org/10.1016/j.cell.2014.03.004 (2014).

9. Sonnenschein, C. & Soto, A. M. Over a century of cancer research: Inconvenient truths and promising leads. *PLoS Biol.* **18**, (2020).

10. Singh, A. *et al.* Are metastatic tumours histologically similar to the primary? Result of a blinded experiment. *medRxiv* 2022–2023 (2023).

11. Fidler, I. J. Metastasis: Quantitative analysis of distribution and fate of tumor emboli labeled with 125l-5-lodo-2'-deoxyuridine. *J. Natl. Cancer Inst.* **45**, (1970).

12. Weiss, L. Metastatic inefficiency. *Adv. Cancer Res.* **54**, 159–211 (1990).

13. Wong, C. W. *et al.* Apoptosis: An early event in metastatic inefficiency. *Cancer Res.* **61**, (2001).

14. Bendich, A., Wilczok, T. & Borenfreund, E. Circulating DNA as a Possible Factor in Oncogenesis. *Science (80-.).* **148**, 374–376 (1965).

15. García-Olmo, D., García-Olmo, D. C., Ontañón, J. & Martinez, E. Horizontal transfer of DNA and the “genometastasis hypothesis”. *Blood* **95**, 724–725 (2000).

16. García-Olmo, D. C. *et al.* Cell-Free Nucleic Acids Circulating in the Plasma of Colorectal Cancer Patients Induce the Oncogenic Transformation of Susceptible Cultured Cells. *Cancer Res.* **70**, 560–567 (2010).

17. Trejo-Becerril, C. *et al.* Cancer Progression Mediated by Horizontal Gene Transfer in an In Vivo Model. *PLoS One* **7**, e52754 (2012).

18. Mittra, I. *et al.* Circulating nucleic acids damage DNA of healthy cells by integrating into their genomes. *J. Biosci.* **40**, 91–111 (2015).

19. Mittra, I. *et al.* Cell-free chromatin from dying cancer cells integrate into genomes of bystander healthy cells to induce DNA damage and inflammation. *Cell Death Discov.* **3**, 1–14 (2017).

20. Hanahan, D. & Weinberg, R. A. Hallmarks of cancer: the next generation. *Cell* **144**, 646–674 (2011).

21. Minn, A. J. *et al.* Distinct organ-specific metastatic potential of individual breast cancer cells and primary tumors. *J. Clin. Invest.* **115**, 44–55 (2005).

22. Kozlowski, J. M., Hart, I. R., Fidler, I. J. & Hanna, N. A human melanoma line heterogeneous with respect to metastatic capacity in athymic nude mice. *J. Natl. Cancer Inst.* **72**, 913–917 (1984).

23. Pilankar, A. *et al.* A pro-oxidant combination of resveratrol and copper down-regulates hallmarks of cancer and immune checkpoints in patients with advanced oral cancer: Results of an exploratory study (RESCU 004). *Front. Oncol.* 5061 (2022).

24. Kim, K. *et al.* Paired Primary and Metastatic Tumor Analysis of Somatic Mutations in Synchronous and Metachronous Colorectal Cancer. *Cancer Res. Treat.* **49**, 161–167 (2017).

25. Vignot, S. *et al.* Comparative analysis of primary tumour and matched metastases in colorectal cancer patients: Evaluation of concordance between genomic and transcriptional profiles. *Eur. J. Cancer* **51**, 791–799 (2015).

26. Lee, S. E., Park, H. Y., Hwang, D.-Y. & Han, H. S. High Concordance of Genomic Profiles between Primary and Metastatic Colorectal Cancer. *Int. J. Mol. Sci.* **22**, 5561 (2021).

27. Roessler, S. *et al.* Integrative Genomic and Transcriptomic Characterization of Matched Primary and Metastatic Liver and Colorectal Carcinoma. *Int. J. Biol. Sci.* **11**, 88–98 (2015).

28. Fang, Q. *et al.* Discordance of epidermal growth factor receptor mutations between primary tumors and corresponding mediastinal nodal metastases in patients operated on for stage N2 non-small cell lung cancer. *Thorac. Cancer* **3**, 313–319 (2012).

29. Kim, E. Y. *et al.* Genetic heterogeneity of actionable genes between primary and metastatic tumor in lung adenocarcinoma. *BMC Cancer* **16**, (2016).

30. Masoodi, T. *et al.* Whole-exome sequencing of matched primary and metastatic papillary thyroid cancer. *Thyroid* **30**, 42–56 (2020).

31. Martínez-Jiménez, F. *et al.* Pan-cancer whole-genome comparison of primary and metastatic solid tumours. *Nature* **618**, 333–341 (2023).

32. Weigelt, B. *et al.* Gene expression profiles of primary breast tumors maintained in distant metastases. *Proc. Natl. Acad. Sci.* **100**, 15901–15905 (2003).

33. Ramaswamy, S., Ross, K. N., Lander, E. S. & Golub, T. R. A molecular signature of metastasis in primary solid tumors. *Nat. Genet.* **33**, 49–54 (2003).

34. Lee, J. Y. *et al.* Gene Expression Profiling of Breast Cancer Brain Metastasis. *Sci. Rep.* **6**, 28623 (2016).

35. Chen, R., Goodison, S. & Sun, Y. Molecular Profiles of Matched Primary and Metastatic Tumor Samples Support a Linear Evolutionary Model of Breast Cancer. *Cancer Res.* **80**, 170–174 (2020).

36. Kaur, J. *et al.* Distinct Gene Expression Profiles of Matched Primary and Metastatic Triple-Negative Breast Cancers. *Cancers (Basel).* **14**, 2447 (2022).

37. Brodsky, A. S. *et al.* Expression Profiling of Primary and Metastatic Ovarian Tumors Reveals Differences Indicative of Aggressive Disease. *PLoS One* **9**, e94476 (2014).

38. Tong, Z. *et al.* Clonal Evolution Dynamics in Primary and Metastatic Lesions of Pancreatic Neuroendocrine Neoplasms. *Front. Med.* **8**, (2021).

39. Dang, H. X. *et al.* The clonal evolution of metastatic colorectal cancer. *Sci. Adv.* **6**, eaay9691 (2020).

40. Wang, Y. *et al.* Clonal evolution in breast cancer revealed by single nucleus genome sequencing. *Nature* **512**, 155–160 (2014).

41. Yates, L. R. *et al.* Genomic Evolution of Breast Cancer Metastasis and Relapse. *Cancer Cell* **32**, 169-184.e7 (2017).

42. Shah, S. P. *et al.* The clonal and mutational evolution spectrum of primary triple-negative breast cancers. *Nature* **486**, 395–399 (2012).

43. Zhang, A. W. *et al.* Interfaces of Malignant and Immunologic Clonal Dynamics in Ovarian Cancer. *Cell* **173**, 1755-1769.e22 (2018).

44. Funnell, T. *et al.* Single-cell genomic variation induced by mutational processes in cancer. *Nature* **612**, 106–115 (2022).

45. Vázquez-García, I. *et al.* Ovarian cancer mutational processes drive site-specific immune evasion. *Nature* **612**, 778–786 (2022).

46. Martin, O. A., Anderson, R. L., Narayan, K. & MacManus, M. P. Does the mobilization of circulating tumour cells during cancer therapy cause metastasis? *Nature Reviews Clinical Oncology* vol. 14 at https://doi.org/10.1038/nrclinonc.2016.128 (2017).

47. Karagiannis, G. S. *et al.* Neoadjuvant chemotherapy induces breast cancer metastasis through a TMEM-mediated mechanism. *Sci. Transl. Med.* **9**, (2017).

48. Monteran, L. *et al.* Chemotherapy-induced complement signaling modulates immunosuppression and metastatic relapse in breast cancer. *Nat. Commun.* **13**, (2022).

49. von Essen, C. F. Radiation enhancement of metastasis: a review. *Clinical & Experimental Metastasis* vol. 9 77–104 at https://doi.org/10.1007/BF01756381 (1991).

50. Vilalta, M., Rafat, M. & Graves, E. E. Effects of radiation on metastasis and tumor cell migration. *Cellular and Molecular Life Sciences* vol. 73 at https://doi.org/10.1007/s00018-016-2210-5 (2016).

51. Demicheli, R., Retsky, M. W., Hrushesky, W. J. M., Baum, M. & Gukas, I. D. The effects of surgery on tumor growth: A century of investigations. *Annals of Oncology* vol. 19 at https://doi.org/10.1093/annonc/mdn386 (2008).

52. Tohme, S., Simmons, R. L. & Tsung, A. Surgery for cancer: A trigger for metastases. *Cancer Research* vol. 77 at https://doi.org/10.1158/0008-5472.CAN-16-1536 (2017).

Acknowledgements

We thank Mr. Ashish Pawar for his help in preparing this manuscript.

Author contributions

G.V.R. designed and performed the experiments, analysed and interpreted the data, and wrote the manuscript. K.P. supervised the experiments and analysed the data. S.S., N.K.K., V.J., S.S., R.P., and H.W. performed the experiments. I.M. conceptualized and designed the project, was responsible for overall supervision and acquisition of funding, interpreted the data, wrote the manuscript, and approved the final draft.

Competing interests

The authors declare no competing interests.

Data availability

All data generated during this study are included in this published article.

Legends to Figures

Fig. 1: Representative images of fluorescently dual-labelled MDA-MB-231 and A-375 cells, and the accumulation of dual-labelled cfChPs in the lung cells of mice following their intravenous injection; **a.** Representative confocal images of fluorescently dual-labelled MDA-MB-231 and A375 cells, in which DNA was labelled with BrdU (red) and histones were labelled with H2B-GFP (green). The extra-nuclear DAPI and BrdU signals represent mitochondrial DNA. **b.** Fluorescence microscopy images showing copious accumulation of dual-labelled particles representing cfChPs in nuclei of lung cells following intravenous injections of dual-labelled MDA-MB-231 and A375 cells at 48 h. One hundred thousand cells were injected intravenously into SCID mice in both the cases.

Fig. 2: Activation of hallmarks of cancer in lung cells of SCID mice following intravenous injection of unlabelled MDA-MB-231 cells at 72 h. One hundred thousand MDA-MB-231 cells were injected intravenously into SCID mice in the experimental group and saline was injected in the control group. Animals were sacrificed at 72 h and cryosections of the lungs were analysed by IF for 13 biomarkers representing 10 hallmarks of cancer; **a.** Histograms representing mean values (± SEM) of the percentage of cells positive for cancer biomarkers in MDA-MB-231-injected and control mice (n=2 in each group). For each biomarker, one thousand cells were analysed and the percentage of positive cells was calculated. The mean (± SEM) values in the control and MDA-MB-231-injected groups were compared using two tailed Student's t test. **b.** Boxplots depicting comparative results of all biomarkers combined together. The median values were compared using the Mann–Whitney U test.

Fig. 3: Co-localisation of mouse and human specific DNA and co-expression of mouse and human specific proteins detected on FFPE sections of lung metastases in MDA-MB-231- and A375-injected mice. **a.** FISH images following simultaneous use of mouse- and human-specific whole genomic probes. Co-localisation of mouse- and human-specific DNA is clearly seen in the metastatic tumour cell nuclei. **b.** IF analysis using mouse and human specific mAbs (MHC-II and HLA-ABC, respectively). Co-expression of MHC-II and HLA-ABC by the same cell is clearly visible in the metastatic tumour cells.

Fig. 4: Detection of chimeric chromosomes in metaphase spreads prepared from cultured cells of MDA-MB-231 and A375 lung metastases. **a.** Metaphase spreads prepared from cells of primary cultures analysed by FISH using human- and mouse-specific DNA probes. **b.** Metaphase spreads prepared from single-cell clones analysed by FISH using human- and mouse-specific DNA probes.

Fig. 5: Co-expression of mouse- and human-specific proteins by the same cells of cultured MDA-MB-231 and A375 lung metastases. **a.** Cells of primary cultures immune-stained with mouse- and human-specific mAbs (MHC-II and HLA-ABC, respectively). **b.** Clones MG6 and AG5 immune-stained with mouse- and human-specific mAbs (MHC-II and HLA-ABC, respectively).

Fig. 6: Co-localisation of mouse- and human-specific DNA and co-expression of mouse- and human-specific proteins detected on FFPE sections of lung metastases that developed following intravenous injection of purified cfChPs isolated from radiation-killed MDA-MB-231 cells. **a.** Co-localisation of mouse- and human-specific DNA; **b.** Co-expression of mouse- and human-specific proteins.

Fig. 7: Graphical illustration of the alternative model of cancer metastasis. CTC = circulating tumour cells. The black dots represent cfChPs.

Figure 1

a

Dually labeled MDA-MB-231 CELLS

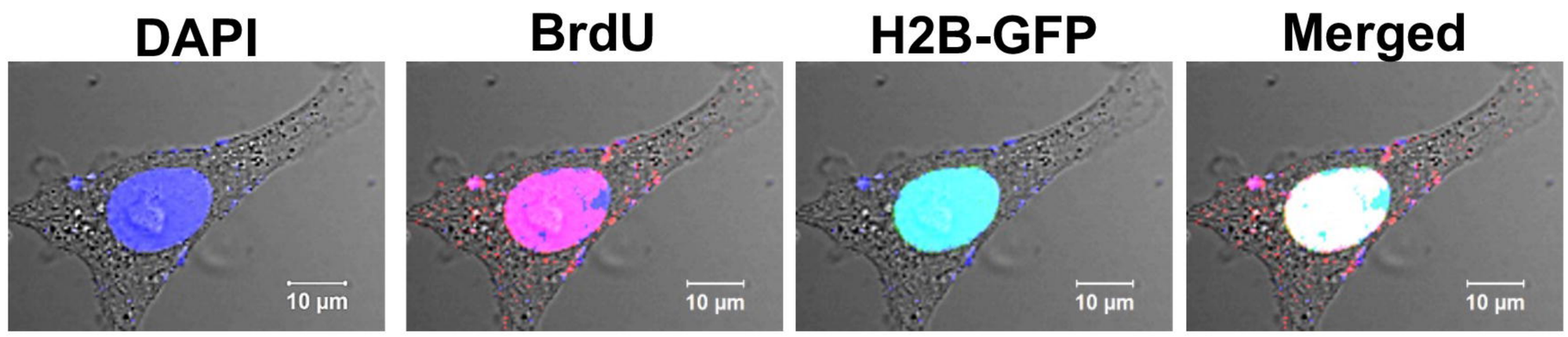

Dually labeled A375 CELLS

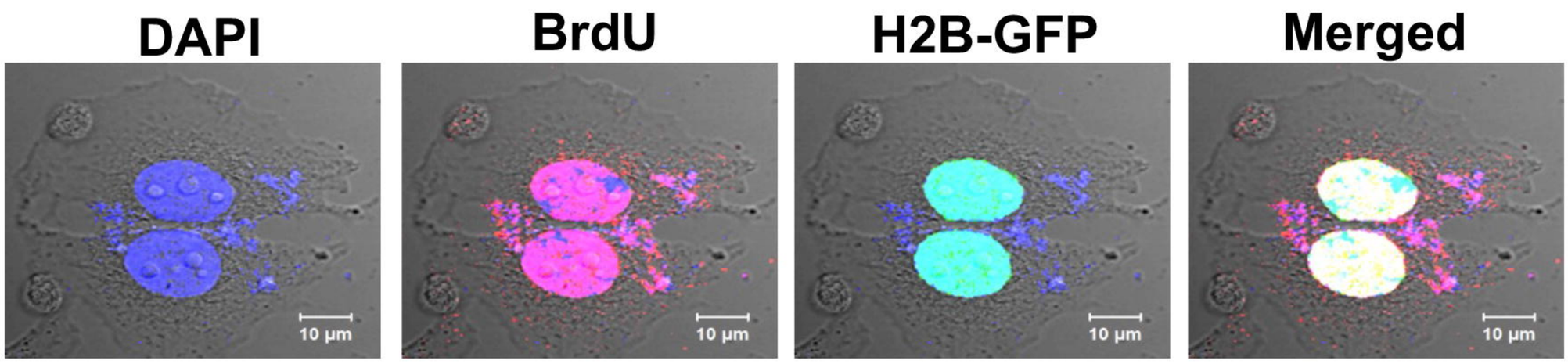

b

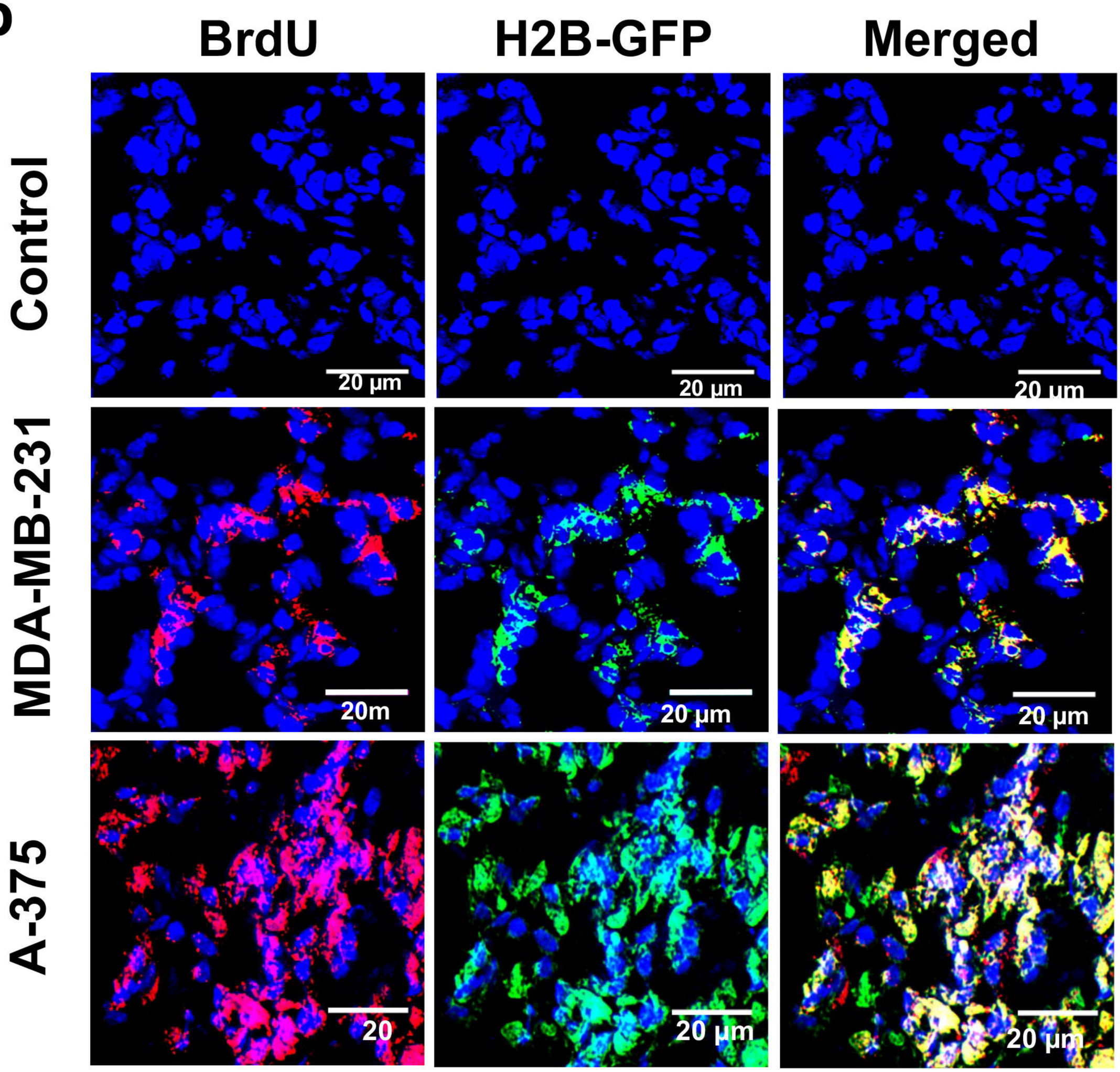

Figure 2

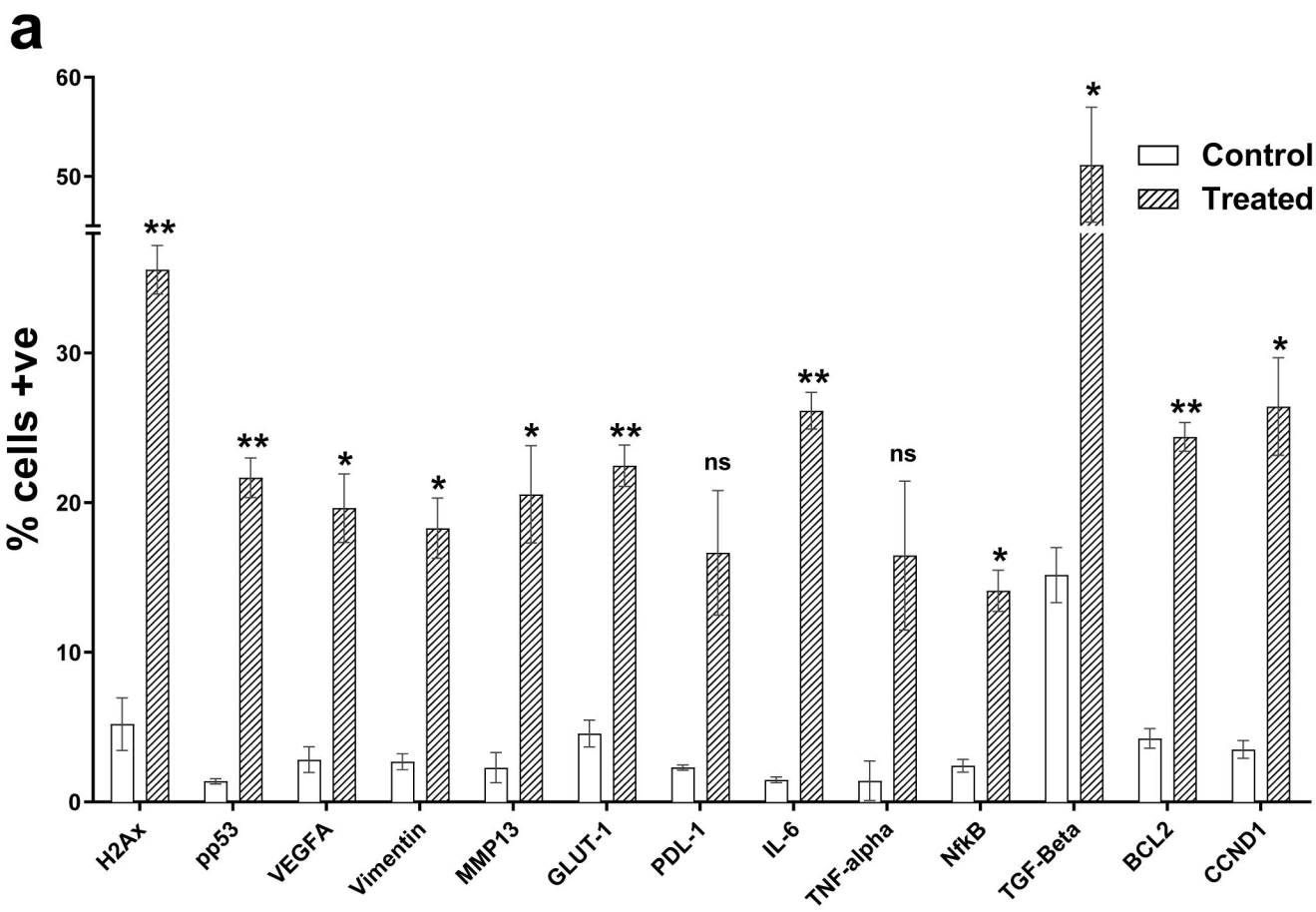
a
% cells +ve
60
50
30
20
10
0
Control
Treated
**
**
*
*
*
**
ns
**
ns
*
*
**
*
H2Ax
pp53
VEGFA
Vimentin
MMP13
GLUT-1
PDL-1
IL-6
TNF-alpha
NfkB
TGF-Beta
BCL2
CCND1

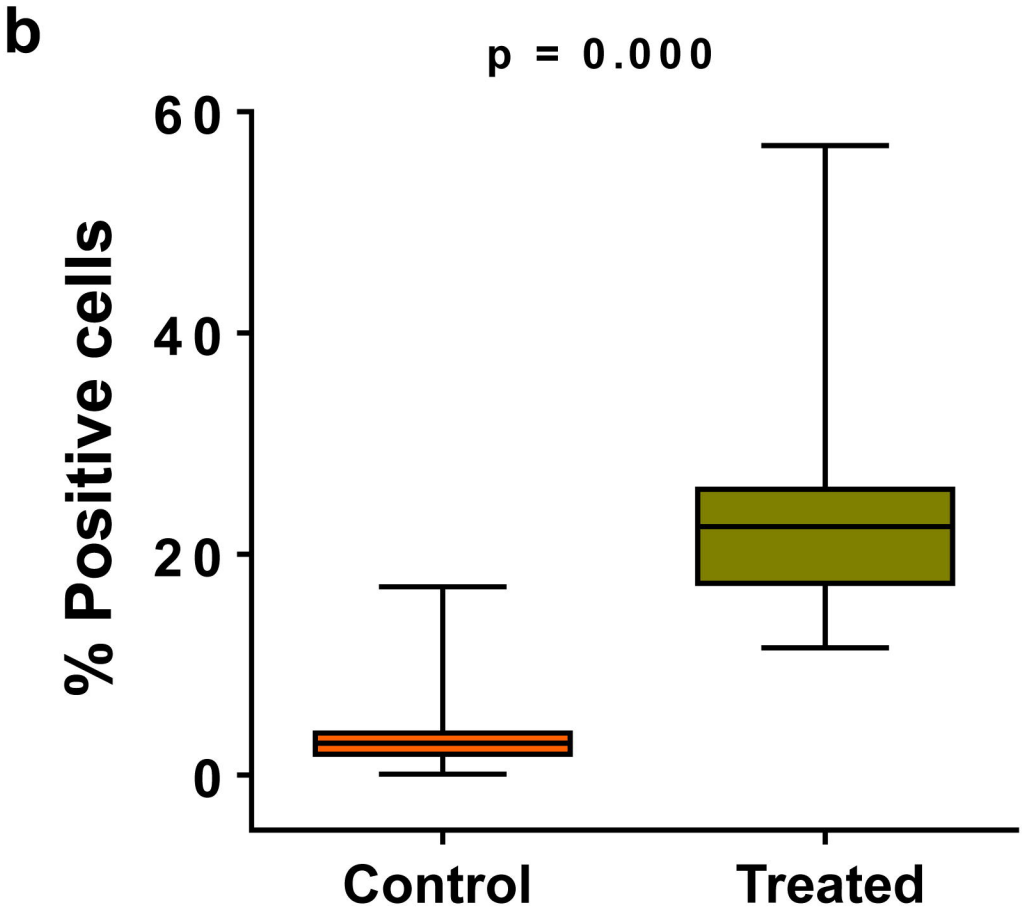
b
p = 0.000
% Positive cells
60
40
20
0
Control
Treated

Figure 3

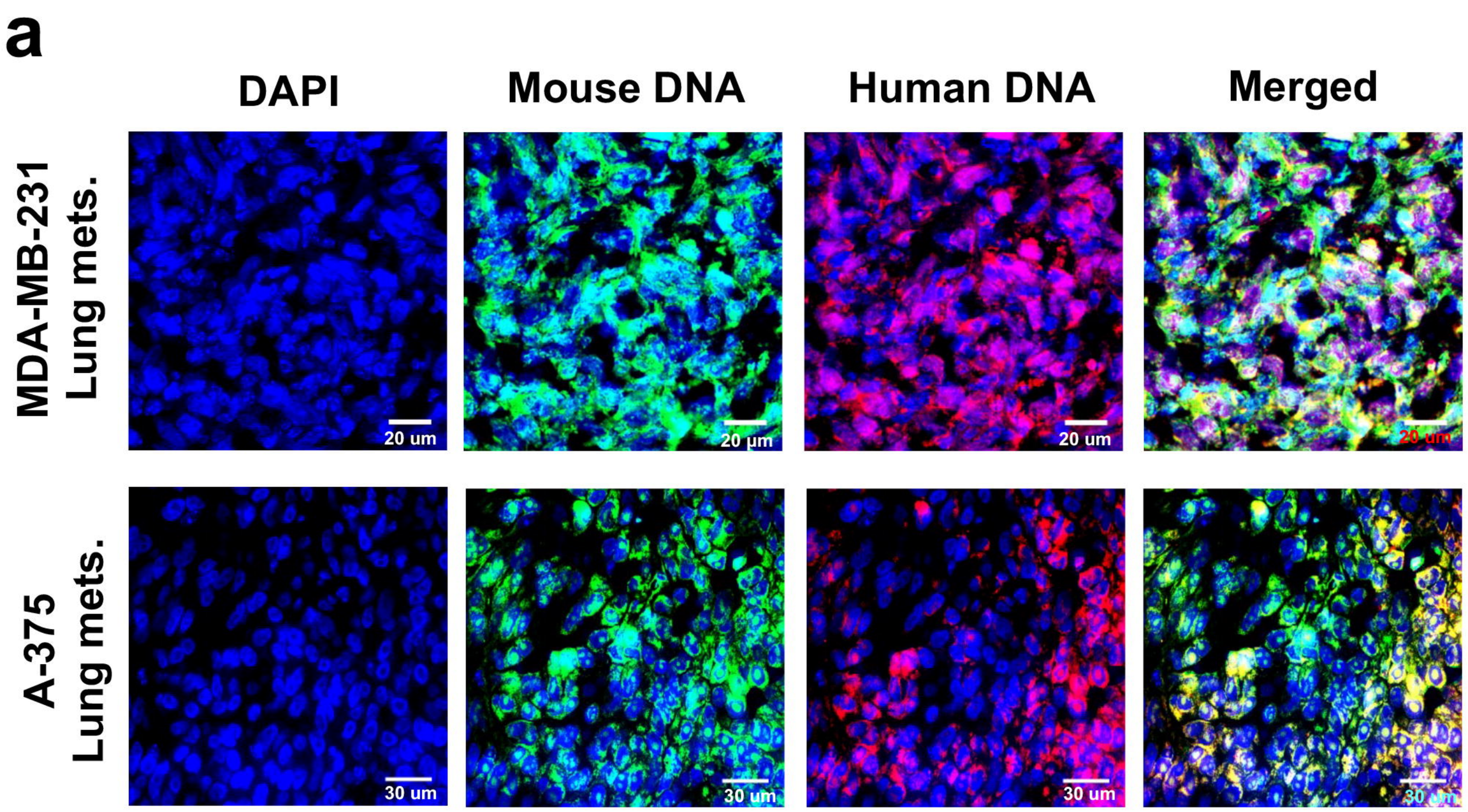
a
DAPI
Mouse DNA
Human DNA
Merged
MDA-MB-231
Lung mets.
A-375
Lung mets.
20 um
20 µm
20 um
20 um
30 um
30 um
30 um
30 um

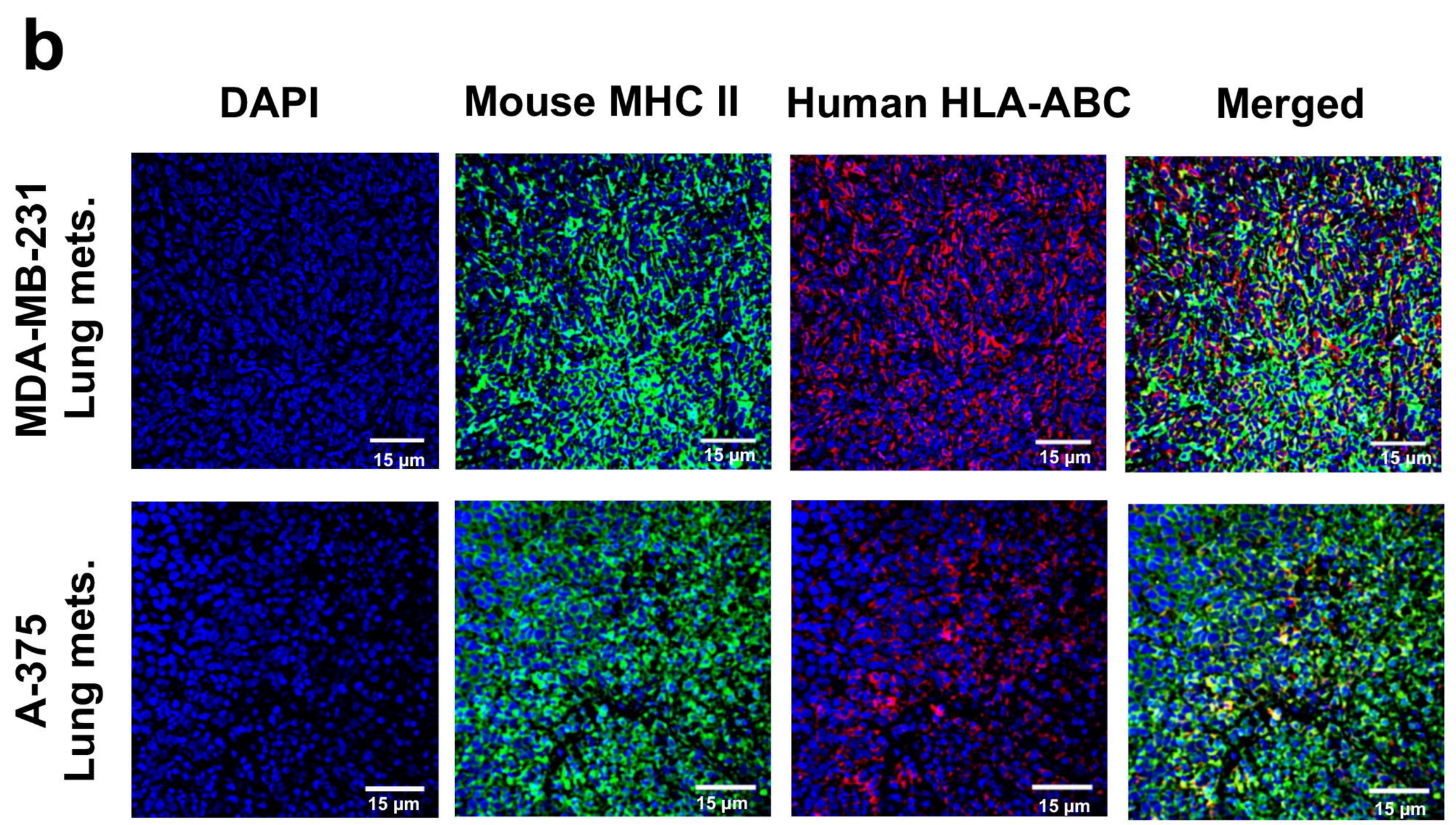
b
DAPI
Mouse MHC II
Human HLA-ABC
Merged
MDA-MB-231
Lung mets.
A-375
Lung mets.
15 µm
15 µm
15 µm
15 µm
15 µm
15 µm
15 µm
15 µm

Figure 4

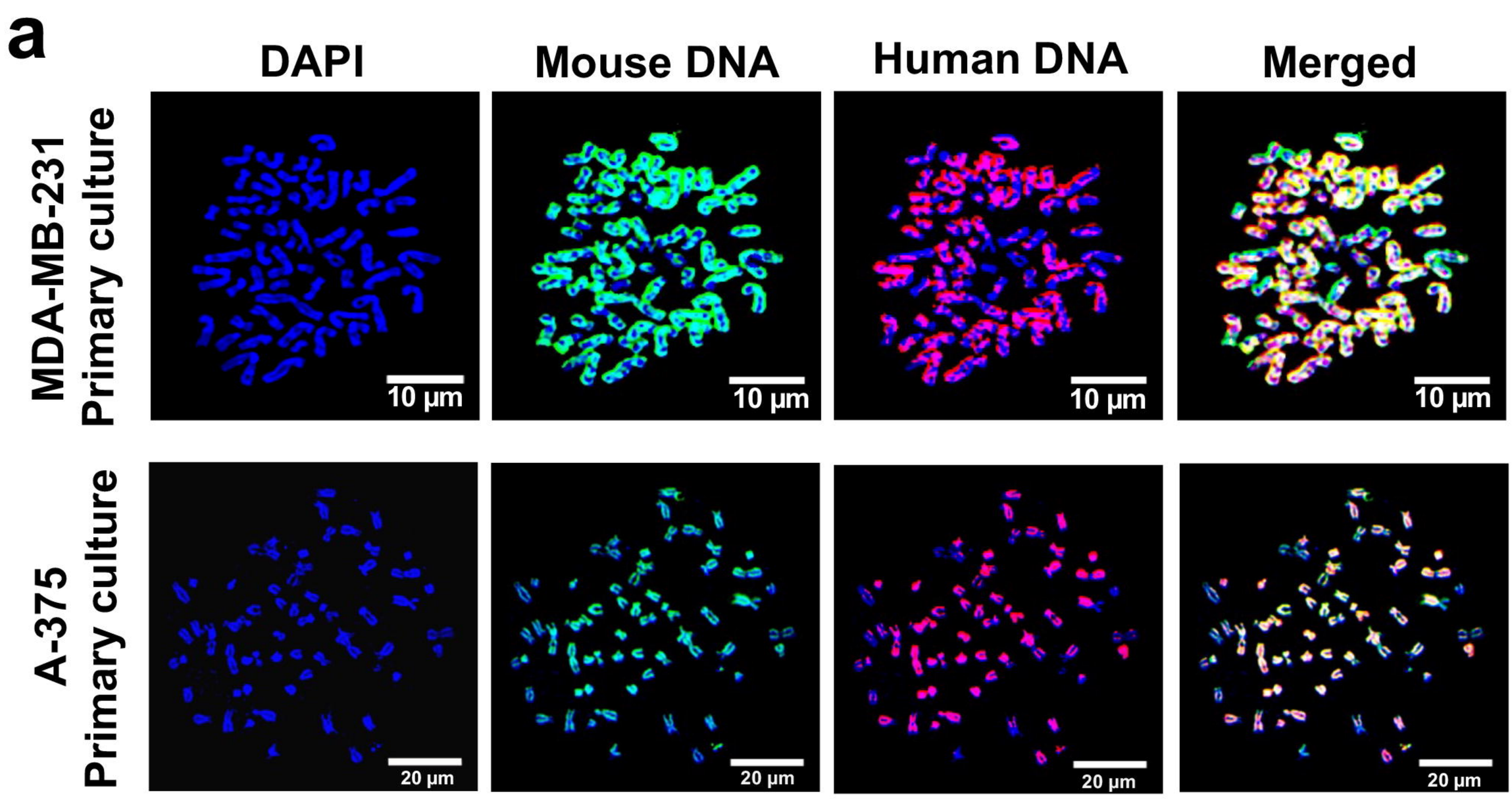
a
DAPI
Mouse DNA
Human DNA
Merged
MDA-MB-231
Primary culture
A-375
Primary culture
10 µm
20 µm

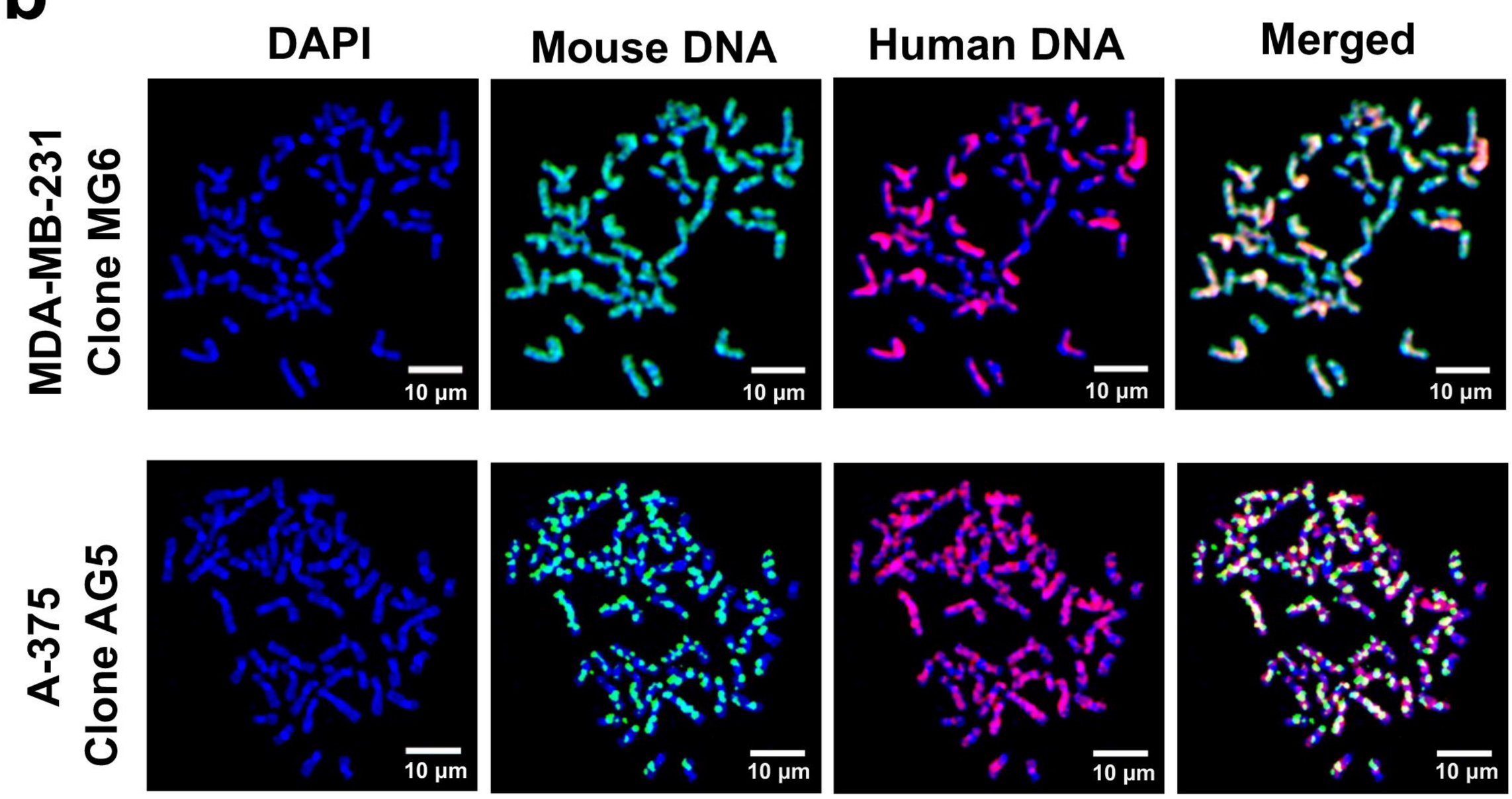
b
DAPI
Mouse DNA
Human DNA
Merged
MDA-MB-231
Clone MG6
A-375
Clone AG5
10 µm

Figure 5

a

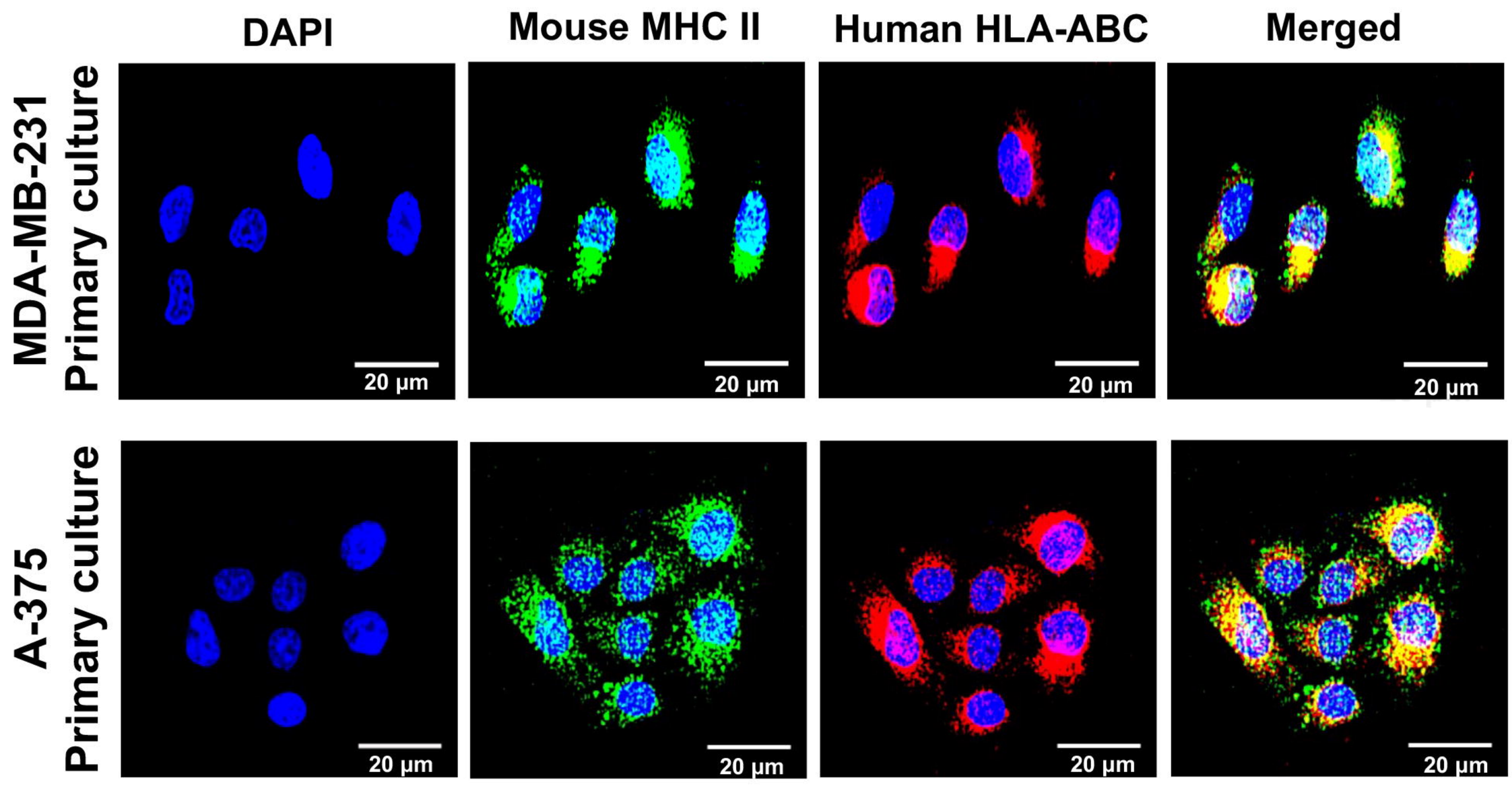
DAPI
Mouse MHC II
Human HLA-ABC
Merged
MDA-MB-231
Primary culture
A-375
Primary culture
20 µm

b

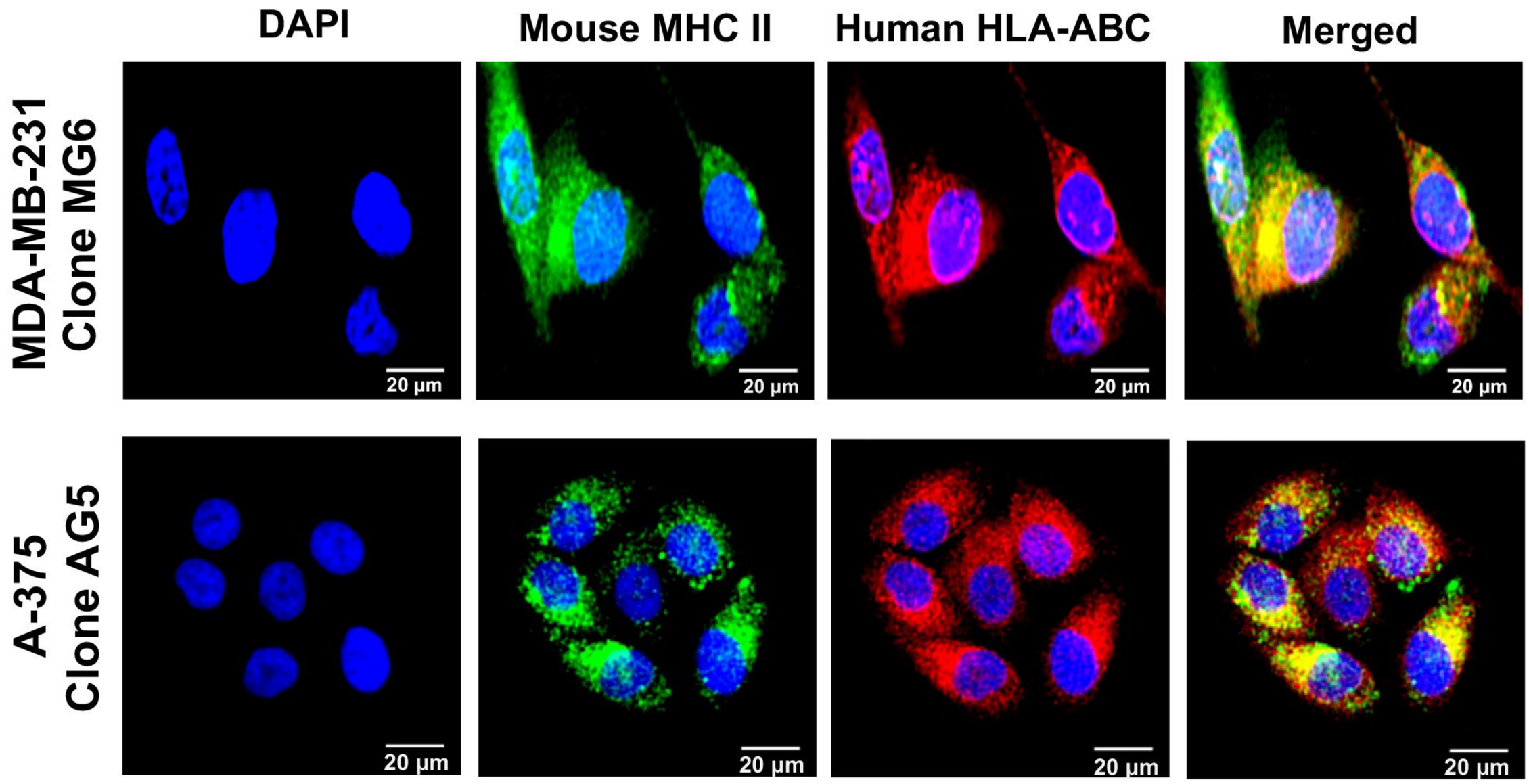
DAPI
Mouse MHC II
Human HLA-ABC
Merged
MDA-MB-231
Clone MG6
A-375
Clone AG5
20 µm

Figure 6

a

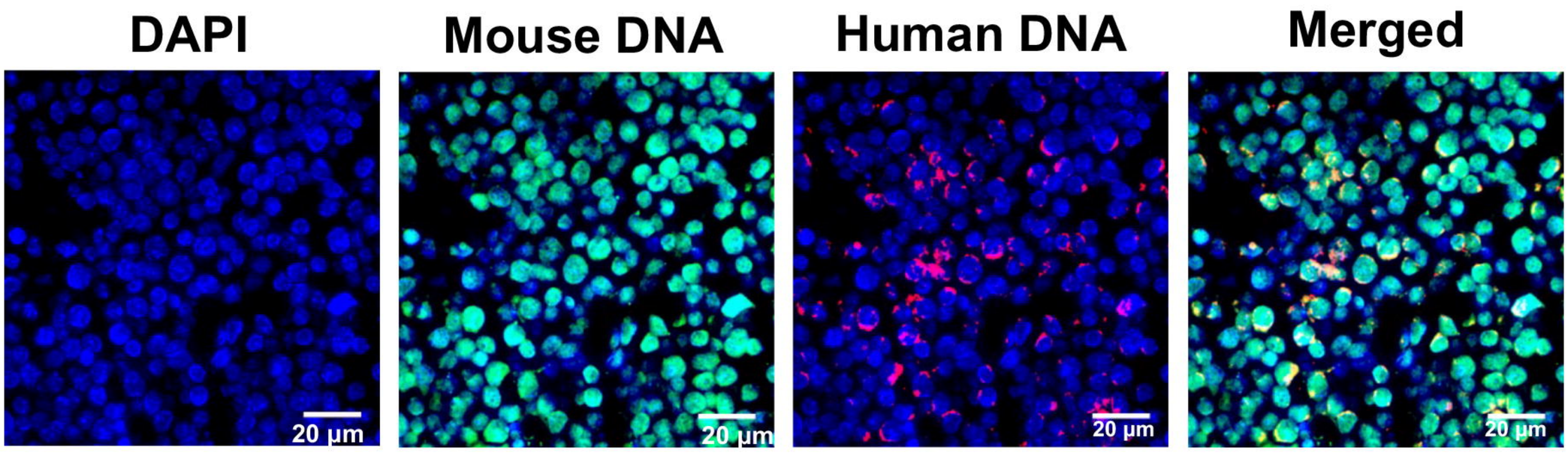
DAPI
Mouse DNA
Human DNA
Merged
20 µm
20 µm
20 µm
20 µm

b

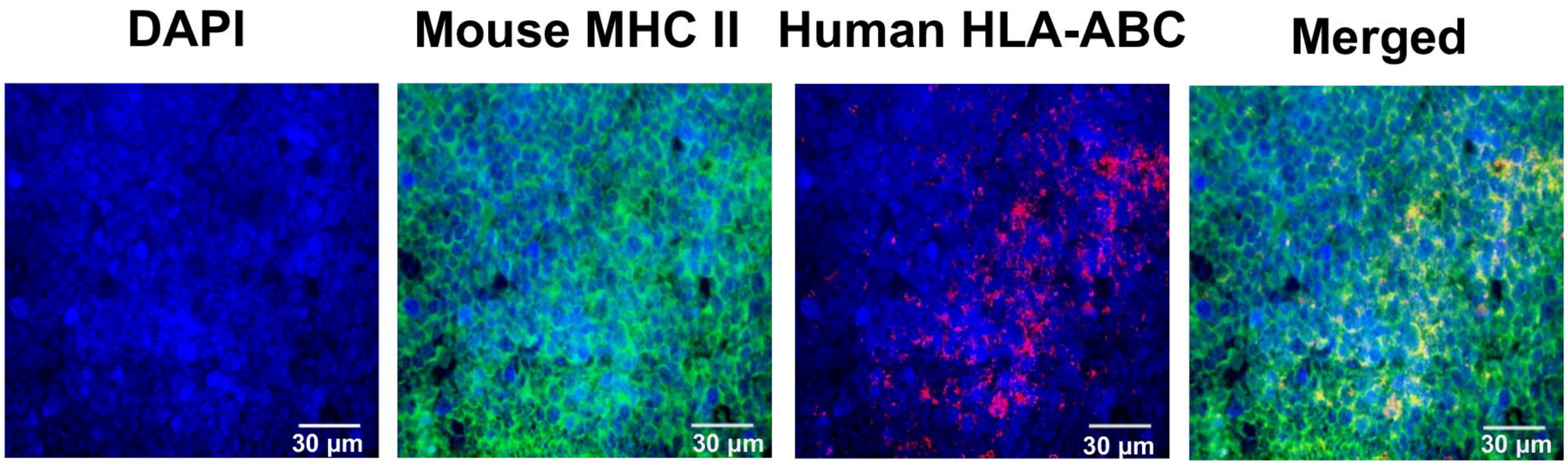
DAPI
Mouse MHC II
Human HLA-ABC
Merged
30 µm
30 µm
30 µm
30 µm
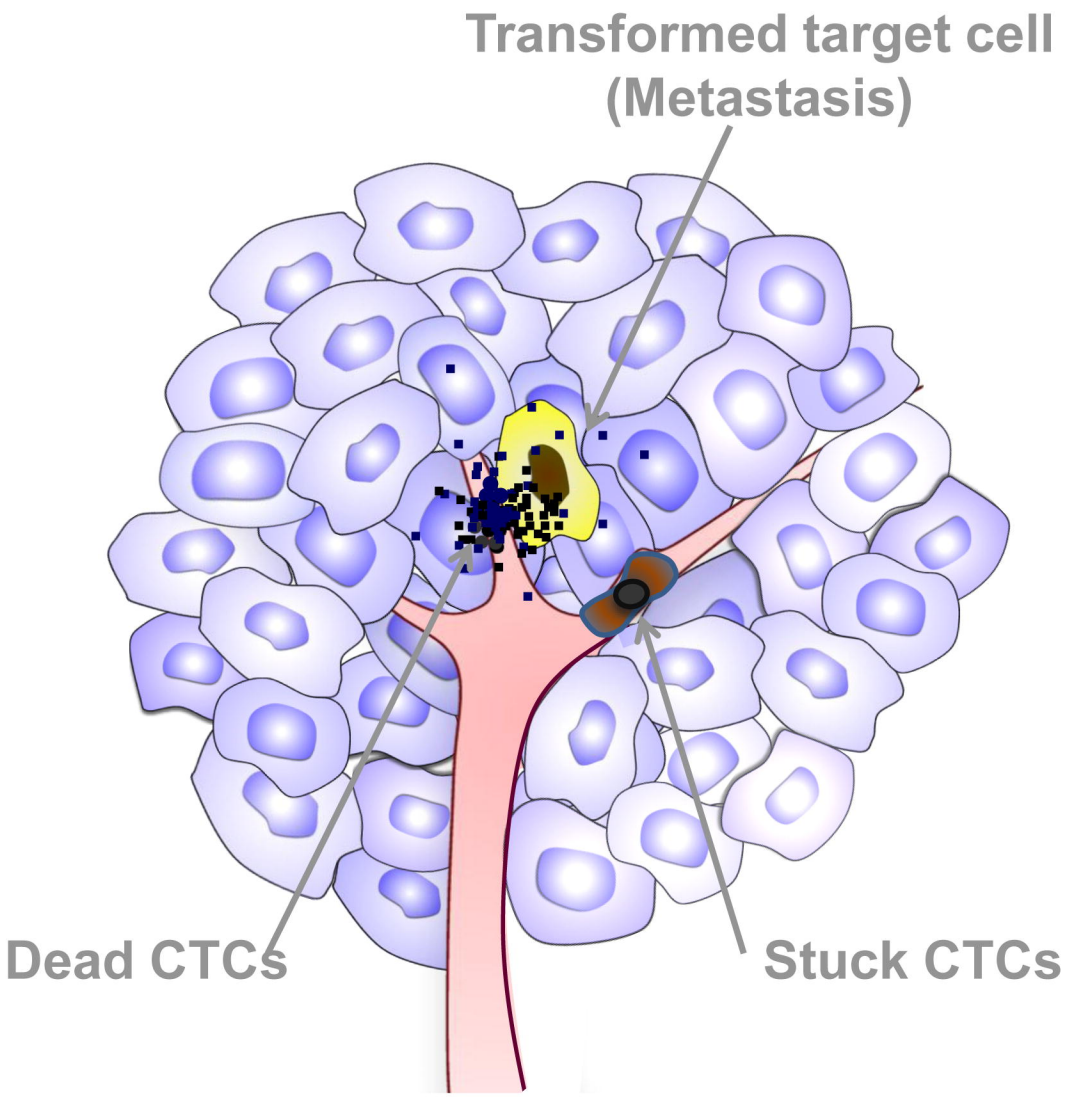
Figure 7